# Truncated Channel Inversion Power Control for the Uplink of mmWave Cellular Networks

Oluwakayode Onireti and Muhammad Ali Imran
School of Engineering, University of Glasgow, Glasgow, UK
Email: {oluwakayode.onireti, muhammad.imran}@glasgow.ac.uk

***Abstract*—In this paper, using the stochastic geometry, we develop a tractable uplink modeling paradigm for the outage probability of millimeter wave (mmWave) cellular networks. Our model takes account of the maximum power limitation and the per-user equipment (UE) power control as well as the effect of blockages. More specifically, each UE, which could be in line-of-sight (LOS) or non-LOS to its serving base station (BS), controls its transmit power such that the received signal power at its serving BS is equal to a predefined threshold. Hence, a truncated channel inversion power control is implemented for the uplink of the mmWave cellular network. We derive expressions for the truncated outage probability and the signal-to-interference-and-noise-ratio (SINR) outage probability for the uplink of mmWave cellular networks. Our results show that contrary to the conventional ultra-high-frequency (UHF) networks there exists a slow growth region for the truncated outage probability.**

***Keywords*—*mmWave, power control, stochastic geometry, truncated channel inversion, uplink communication.***

## I. Introduction

Extreme network densification, massive multiple-input-multiple-output (MIMO) and increased bandwidth have been identified as the key approaches toward meeting the increased data rate requirement of 5G networks. With the limited bandwidth in the microwave spectrum, the millimeter wave (mmWave) band ranging from $30 - 300$ GHz are now been considered for the future 5G cellular networks. However, such frequency bands have long been deemed unsuitable for cellular communications as a result of the large free space pathloss and poor penetration (i.e., blockage effect) through materials such as water, concrete, etc. Only recently did survey measurements and capacity studies of mmWave technology reveal its promise for urban small cell deployments [1]–[4]. In addition to the huge available bandwidth in the mmWave band, the smaller wavelength associated with the band combined with recent advances in low-power CMOS RF circuits have paved the way for the use of more miniaturized antennas at the same physical area of the transmitter and receiver to provide array gain [4], [5]. With such a large antenna array, the mmWave cellular system can apply beamforming at the transmit and receive sides to provide array gain which compensates for the near-field pathloss [6]. Further, the directionality gained from beamforming will lead to a reduction in interference as compared with the conventional ultra-high-frequency (UHF) networks [3]. Hence, mmWave spectrum holds great potential for providing the high data rate (Gigabits range) expected in the upcoming 5G cellular networks [7].

Recently, use of stochastic geometry-based analysis was extended to the uplink of a single tier UHF cellular networks in [8]. The authors took in to account the per-user equipment (UE) fractional power control but did not incorporate the limitation in the UE transmit power in their framework. In [9]–[11], the authors developed the stochastic geometry framework for the uplink of a multi-tier UHF cellular network while taking account of the limitation in the UE transmit power through a predefined cut-off threshold. In addition, the truncation outage probability for the uplink a multi-tier UHF cellular network was presented in [9], [11]. The authors in [11] also addressed energy efficiency in the uplink channel under the maximum power constraint.

In mmWave networks, blockages result in a significant difference between the line-of-sight (LOS) and non-line-of-sight (NLOS) pathloss characteristics. The measurements showed that mmWave signals propagate with a pathloss exponent of 2 in LOS paths and a much higher pathloss exponent with additional shadowing in NLOS paths [1], [2]. Typical measured values of the NLOS pathloss exponent range from 3.2 to 5.8 [1], [2]. This poses a challenge in the uplink propagation since the difference in pathloss exponents could results in excessive interference from NLOS UEs when fraction power control is implemented. In order to address this issue, we have proposed a distance based fractional power control scheme for the uplink of mmWave networks in [12], [13]. However, our analysis did not consider the limitation in the UE transmit power.

In this paper, we present a stochastic geometry framework which takes into account the limitation in the UE transmit power, the per-UE power control and the cutoff threshold for the power control. Hence, we here extend the work in [12], [13] which did not take into account the maximum transmit power of the UE in addition to imposing an unbounded pathloss. The rest of the paper is organized as follows. The system model and methodology of our analysis are presented in Section II. In Section III, we present the transmission power analysis and the derivation of the truncation outage probability. Section IV presents the SINR outage probability with a cutoff threshold. Numerical results are presented in Section V and the paper is concluded in Section VI.

## II. System Model

We consider the uplink of a mmWave cellular network and focus on the SINR experienced by outdoor users served by outdoor base stations (BSs). The outdoor BSs are spatially distributed in $\mathbb{R}^2$ according to an independent homogeneous Poisson point process (PPP) with density $\lambda$. The user locations (before association) are assumed to form a realization of homogeneous PPP with density $\lambda_u$. Each BS serves a single user per channel, which is randomly selected from all the users located in its Voronoi cell by using a round-robin scheduler. Hence, the user PPP $\lambda_u$ is thinned to obtain a point process $\Phi = \{X_z\}$, where $X_z$ is the location of active outdoor users.

As in [9], [14], we assume that the active users also form PPP even after associating just one user per BS. Since we have one active user per cell, the density $\phi$ of the thinned PPP of active users is set to be equal to the BS density $\lambda$. The mmWave network is characterized by a non-negative blockage constant $\beta$, which is determined by the average size and density of blocakges and where the average line-of-sight (LOS) range is given by $\frac{1}{\beta}$ [7], [15]. The probability of a communication link with length $r$ being a LOS is $\mathbb{P}(\text{LOS}) = e^{-\beta r}$, while the probability of a link being NLOS is $\mathbb{P}(\text{NLOS}) = 1 - \mathbb{P}(\text{LOS})$. The LOS and NLOS links will have different pathloss exponent $\alpha_L$ and $\alpha_N$, respectively. All UEs and BSs are equipped with directional antennas with sectorized gain pattern. The main lobe gain, side lobe gain and beamwidth of the UE are $G_u^{\max}$, $G_u^{\min}$ and $\kappa_t$, while the corresponding parameters of the BS antennas are $G_b^{\max}$, $G_b^{\min}$ and $\kappa_r$. We consider that based on channel estimation, the reference BS and the typical user adjust their beam steering angles to achieve the maximum array gains. As a result of this, the total directivity gain of the desired signal is $G_b^{\max} G_u^{max}$. Furthermore, the directivity gain in the interference link $G_l$ can be approximated as discrete random variable whose probability distribution is given as $a_k$ with probability $b_k$ ($k \in \{1,2,3,4\}$), where $a_1 = G_b^{\max} G_u^{\max}$, $b_1 = \frac{\kappa_r \kappa_t}{4\pi^2}$, $a_2 = G_b^{\max} G_u^{\min}$, $b_2 = \frac{\kappa_r}{2\pi}(1 - \frac{\kappa_t}{2\pi})$, $a_3 = G_b^{\min} G_u^{\max}$, $b_3 = (1 - \frac{\kappa_r}{2\pi})\frac{\kappa_t}{2\pi}$, $a_4 = G_b^{\min} G_u^{\min}$ and $b_4 = (1 - \frac{\kappa_r}{2\pi})(1 - \frac{\kappa_t}{2\pi})$ [7].

Furthermore, all BS are assumed to have equal receiver sensitivity $\rho_{\min}$. To achieve a successful uplink transmission, the received signal at the BS must be greater than the receiver sensitivity. As a result, each UE (with either LOS or NLOS link to serving BS) controls its transmit power such that the average signal received at the serving BS is equal to a predefined threshold $\rho_o$, where $\rho_o > \rho_{\min}$. We assume that all UEs have an equal maximum transmit power, $P_u$. Hence, as a result of the transmit power constraint for uplink transmission, each UE utilizes a truncated channel inversion power control. In this scheme, the transmitters compensate for the pathloss in the link to the receiver to keep the average received signal power to the threshold $\rho_o$. Consequently, the connection between the UE and the BS will be established if and only the transmission power required for the channel (pathloss) inversion is less than $P_u$. Otherwise, the UE does not transmit and goes into a truncated outage due the insufficient transmit power [9].

## III. mmWave Transmission Power Analysis

Considering the random network topology together with the blockage effect and the truncated channel inversion scheme, each UE will transit with different power to invert the pathloss towards its serving BS (LOS/NLOS). As a result of the truncation channel inversion, not all UEs will be able to communicate in the uplink channel when the cutoff threshold $\rho_o$ is high relative to $\lambda$ and $P_u$. Given the cutoff threshold $\rho_o$, LOS and NLOS UEs located at distances greater than $(Pu/\rho_o)^{1/\alpha_L}$ and $(Pu/\rho_o)^{1/\alpha_N}$, respectively, from their nearest BS are unable to communicate in the uplink direction due to insufficient transmit power. Hence, in addition to the fact that the complete set of UEs are divided into a subset of LOS and NLOS users based on their association with their serving BS, the LOS and NLOS UE sets are further divided into a non-overlapping subset of active UEs and inactive UEs. The distribution of the transmit power of a typical UE is obtained from the following lemma.

*Lemma 3.1:* In mmWave cellular networks with truncated channel inversion power control and cutoff threshold $\rho_o$, the probability distribution function (PDF) of the transmit power of a typical UE in the uplink is given by

$$f_P(x, \rho_o, \lambda, \beta, P_u) = \frac{\gamma(x, \rho_o, \lambda, \beta) e^{-\Gamma(x, \rho_o, \lambda, \beta)}}{\int_0^{P_u} \gamma(x, \rho_o, \lambda, \beta) e^{-\Gamma(x, \rho_o, \lambda, \beta)}}, \quad (1)$$

where

$$\gamma(x, \rho_o, \lambda, \beta) = \frac{2\pi\lambda}{\alpha_L \rho_o^{2/\alpha_L}} x^{\frac{2}{\alpha_L} - 1} e^{-\beta\left(\frac{x}{\rho_o}\right)^{\frac{1}{\alpha_L}}} + \frac{2\pi\lambda}{\alpha_N \rho_o^{2/\alpha_N}} x^{\frac{2}{\alpha_N} - 1} \left(1 - e^{-\beta\left(\frac{x}{\rho_o}\right)^{\frac{1}{\alpha_N}}}\right) \quad (2)$$

and

$$\Gamma(x, \rho_o, \lambda, \beta) = \frac{2\pi\lambda}{\beta^2}\left(1 - e^{-\beta\left(\frac{x}{\rho_o}\right)^{\frac{1}{\alpha_L}}}\left(1 + \beta\left(\frac{x}{\rho_o}\right)^{\frac{1}{\alpha_L}}\right)\right) + \pi\lambda\left(\frac{x}{\rho_o}\right)^{\frac{2}{\alpha_N}} - \frac{2\pi\lambda}{\beta^2}\left(1 - e^{-\beta\left(\frac{x}{\rho_o}\right)^{\frac{1}{\alpha_N}}}\left(1 + \beta\left(\frac{x}{\rho_o}\right)^{\frac{1}{\alpha_N}}\right)\right). \quad (3)$$

*Proof:* The proof follows directly from [16] and is omitted here. Note that the PDF of $P$ has been normalized due to the use of a truncated channel inversion power control. ■

From Lemma 3.1, the $\eta^{th}$ moment of the transmit power obtained as

$$\mathbb{E}\left[P^{\eta}\right] = \int_0^{P_u} x^{\eta} f_P(x, \rho_o, \lambda, \beta, P_u) \mathrm{d}x, \quad (4)$$

where $f_P(x, \rho_o, \lambda, \beta, P_u)$ is given in (1). Further, the truncation outage probability, which is the probability that a UE experience outage due to insufficient power, is expressed as

$$\mathcal{O}_p = e^{-\Gamma(P_u, \rho_o, \lambda, \beta)}, \quad (5)$$

where $\Gamma(v, \rho_o, \lambda, \beta)$ is given in (3).

## IV. SINR Outage Probability

For an active typical UE, the SINR at its connected BS (termed as the reference BS) can be written as

$$SINR = \frac{\rho_o |g_o|^2 G_b^{\max} G_u^{\max}}{\sigma^2 + \sum_{z \in \mathcal{Z}} P_z |g_z|^2 G_z L(D_z)}, \quad (6)$$

where the useful signal power (normalized by $G_b^{\max} G_u^{\max}$) is equal to $\rho_o |g_o|^2$ due to the truncated channel inversion power control, $\mathcal{Z}$ is the set of interfering users, $L(D_z)$ is the pathloss from the interfering user to the reference BS, $\sigma^2$ is the noise power, $G_z$ is the directivity gain on an interfering link and $g_z$ is the small scale fading which follows a Nakagami distribution with parameter $N$. The SINR outage probability can be obtained from the following theorem.

*Theorem 4.1:* The SINR outage probability in the uplink of mmWave cellular networks with truncated channel inversion power control can be expressed as

$$\mathcal{O}_s = 1 - \sum_{n=1}^{N} (-1)^{n+1} \binom{N}{n} \exp\left(-sn\sigma^2 - Q_n - V_n\right) \quad (7)$$

where

$$Q_n = 2\pi\lambda \sum_{k=1}^{4} b_k q_k^{\frac{2}{\alpha_L}} \times \int_{\mathcal{A}}^{\infty} \int_0^{P_u} \mathcal{F}\left(N, \frac{y^{-\alpha_L}}{N}\right) e^{-\beta (q_k P)^{\frac{1}{\alpha_L}} y} y P^{\frac{2}{\alpha_L}} f_P \mathrm{d}P \mathrm{d}y, \quad (8)$$

$$V_n = 2\pi\lambda \sum_{k=1}^{4} b_k q_k^{\frac{2}{\alpha_N}} \times \int_{\mathcal{B}}^{\infty} \int_{0}^{P_u} \mathcal{F}\left(N, \frac{y^{-\alpha_N}}{N}\right) \left(1 - e^{-\beta (q_k P)^{\frac{1}{\alpha_N}} y}\right) y P^{\frac{2}{\alpha_N}} f_P \mathrm{d}P\mathrm{d}y, \quad (9)$$

where $s = \frac{\eta\theta}{\rho_o \mathcal{G}}$, $\eta = N(N!)^{-\frac{1}{N}}$, $\mathcal{G} = G_u^{\max} G_b^{\max}$, $\mathcal{A} = (sna_k\rho_o)^{-\frac{1}{\alpha_L}}$, $\mathcal{B} = (sna_k\rho_o)^{-\frac{1}{\alpha_N}}$, $\mathcal{F}(N,y) = 1 - \frac{1}{(1+y)^N}$, $q_k = sna_k$, $a_k$ and $b_k$ are the antenna directivity parameters defined in Section II and $f_P$ is defined in (1).

*Proof:* Given that the average received signal at the reference BS (normalized by the directivity gain $G_b^{\max} G_u^{\max}$) is equal to the cutoff threshold $\rho_o$. The SINR outage probability can be computed as

$$\mathbb{P}(SINR \leq \theta) = \mathbb{P}\{\rho_o |g_o|^2 \mathcal{G} \leq \theta(\sigma^2 + I_L + I_N)\}, \quad (10)$$

where $I_L$ and $I_N$ are the interference strength from LOS and NLOS users, respectively, and $\mathcal{G} = G_b^{\max} G_u^{\max}$. Noting that $|g_o|^2$ is normalized gamma random variable with parameter $N$, we have the following approximation

$$\begin{aligned}
&\mathbb{P}\{|g_o|^2 \leq \theta(\sigma^2 + I_L + I_N)/(\rho_o \mathcal{G})\} \quad (11)\\
&\overset{(a)}{\approx} 1 - \left(1 - \mathbb{E}\left[\left(1 - e^{-\frac{\eta\theta\left(\sigma^2 + I_L + I_N\right)}{\rho_o \mathcal{G}}}\right)^N\right]\right)\\
&\overset{(b)}{=} 1 - \sum_{n=1}^{N} (-1)^{n+1} \binom{N}{n} \mathbb{E}_{\Phi}\left[e^{-\frac{n\eta\theta\left(\sigma^2 + I_L + I_N\right)}{\rho_o \mathcal{G}}}\right]\\
&= 1 - \sum_{n=1}^{N} (-1)^{n+1} \binom{N}{n} e^{-sn\sigma^2} \mathbb{E}_{\Phi_L}\left[e^{-snI_L}\right] \mathbb{E}_{\Phi_N}\left[e^{-snI_N}\right],
\end{aligned}$$

where $s = \frac{\eta\theta}{\rho_o \mathcal{G}}$, $\eta = N(N!)^{-\frac{1}{N}}$, $(a)$ follow from the fact that $|g_0|^2$ is a normalized gamma random variable with parameter $N$ and the fact that for a constant $\gamma > 0$, the probability $\mathbb{P}(|g_0|^2 < \gamma)$ is tightly upper bounded by $\left[1 - \exp\left(-\gamma N (N!)^{-\frac{1}{N}}\right)\right]^N$ [17]. $(b)$ follows from the binomial theorem and the assumption that $N$ is an integer. Noting that the average interference received from any interfering user (normalized by $\mathcal{G}$) is strictly less than $\rho_o$. Consequently, the sum interference received at the reference BS from LOS interferers can be expressed from (6) as

$$I_L = \sum_{u_z \in \Phi_L \setminus \{o\}} \mathbb{1}\left(P_z \|u_z\|^{-\alpha_L} < \rho_o\right) P_z G_z |g_z|^2 \|u_z\|^{-\alpha_L} \quad (12)$$

where $\Phi_L$ is a PPP of LOS interferers, and $\mathbb{1}(.)$ is an indicator function which takes the values of one when $(.)$ is true and zero otherwise. Consequently, the term of the LOS interferer link $\mathbb{E}_{\Phi_L}\left[e^{-snI_L}\right]$ in (11) can be computed as

$$\begin{aligned}
&\mathbb{E}_{\Phi_L}\left[e^{-snI_L}\right] \quad (13)\\
&= \mathbb{E}_{\Phi_L}\left[e^{-sn\sum_{u_z \in \Phi_L \setminus \{o\}} \mathbb{1}\left(P_z \|u_z\|^{-\alpha_L} < \rho_o\right) P_z G_z |g_z|^2 \|u_z\|^{-\alpha_L}}\right]\\
&\overset{(c)}{=} \mathbb{E}_{P_z, g_z, G_z}\left[\prod_{u_z \in \Phi_L \setminus \{o\}} e^{-sn\mathbb{1}\left(\|u_z\| > \left(\frac{P_z}{\rho_o}\right)^{\frac{1}{\alpha_L}}\right) P_z G_z |g_z|^2 \|u_z\|^{-\alpha_L}}\right]\\
&\overset{(d)}{=} e^{\left(-2\pi\lambda \sum_{k=1}^{4} b_k \int_{\left(\frac{P}{\rho_o}\right)^{\frac{1}{\alpha_L}}}^{\infty} \mathbb{E}_{P,g}\left[\left(1 - e^{-sna_k P g r^{-\alpha_L}}\right)\right] r e^{-\beta r} \mathrm{d}r\right)}\\
&\overset{(e)}{=} e^{\left(-2\pi\lambda \sum_{k=1}^{4} b_k \int_{\left(\frac{P}{\rho_o}\right)^{\frac{1}{\alpha_L}}}^{\infty} \mathbb{E}_{P}\left[\left(1 - \frac{1}{\left(1 + sna_k P r^{-\alpha_L}/N\right)^N}\right)\right] r e^{-\beta r} \mathrm{d}r\right)}\\
&= \prod_{k=1}^{4} e^{-2\pi\lambda b_k \int_{\left(\frac{P}{\rho_o}\right)^{\frac{1}{\alpha_L}}}^{\infty} \mathbb{E}_{P}\left[\left(1 - \frac{1}{\left(1 + sna_k P r^{-\alpha_L}/N\right)^N}\right) r e^{-\beta r}\right] \mathrm{d}r}\\
&\overset{(f)}{=} \prod_{k=1}^{4} e^{-2\pi\lambda q_k^{\frac{2}{\alpha_L}} b_k \int_{\mathcal{A}}^{\infty} \int_{0}^{P_u} \left(1 - \frac{1}{\left(1 + \frac{y^{-\alpha_L}}{N}\right)^N}\right) y P^{\frac{2}{\alpha_L}} e^{-\beta (q_k P)^{\frac{1}{\alpha_L}} y} f_P \mathrm{d}P\mathrm{d}y}\\
&= e^{-Q_n},
\end{aligned}$$

where $(c)$ follows from the independence of $\Phi_L$, $g_z$, $G_z$ and $P_z$, $(d)$ follows from the probability generation functional (PGFL) of the PPP [18] and the independence of the interference link directivity gain $G_z$ with probability distribution $G_z = a_k$ with probability $b_k$, $(e)$ follows from from computing the moment generating function of a gamma random variable $g$, $(f)$ is obtained by changing the variables $y = r/(sna_k P)^{\frac{1}{\alpha_L}}$ while $f_P$ is given in (1). Further, $\mathcal{A} = (sna_k\rho_o)^{-\frac{1}{\alpha_L}}$ and $q_k = sna_k$. Similarly, the for the NLOS interfering links, $\mathbb{E}_{\Phi_N}\left[e^{-nsI_N}\right]$ can be computed as

$$\begin{aligned}
&\mathbb{E}_{\Phi_N}\left[e^{-nsI_N}\right] \quad (14)\\
&= \prod_{k=1}^{4} e^{-2\pi\lambda q_k^{\frac{2}{\alpha_N}} b_k \int_{\mathcal{B}}^{\infty} \int_{0}^{P_u} \left(1 - \frac{1}{\left(1 + \frac{y^{-\alpha_N}}{N}\right)^N}\right) y P^{\frac{2}{\alpha_N}} Z(y,p) f_P \mathrm{d}P\mathrm{d}y}\\
&= e^{-V_n},
\end{aligned}$$

where $\mathcal{B} = (sna_k\rho)^{-\frac{1}{\alpha_N}}$ and $Z(y,p) = \left(1 - e^{-\beta (q_k P)^{\frac{1}{\alpha_N}} y}\right)$. ■

## V. Numerical Results

In this section, we present some numerical results to illustrate our analytical findings. The LOS and NLOS pathloss exponents are taken as $\alpha_L = 2$ and $\alpha_N = 4$, respectively. Unless otherwise stated, the blockage parameter $\beta = 0.0071$, the Nakagami fading parameter $N = 3$, the antenna gain pattern of a BS is assumed to be characterized with $G_b^{\max} = 10$ dB, $G_b^{\min} = -10$ dB and $\kappa_b = 30°$, while that of a user is assumed to be characterized with $G_u^{\max} = 10$ dB, $G_u^{\min} = -10$ dB and $\kappa_u = 90°$.

Fig. 1 compares the truncation outage probability for the uplink of mmWave and UHF cellular networks for BS density $\lambda = 1, 10$ and $100$ BS/km$^2$. The truncation outage probability of UHF networks has been defined in [9]. It can be seen that similar to the UHF case, increasing the cutoff threshold increases the outage probability since more UEs are unable to communicate due to insufficient transmit power. Furthermore, for BS densities $\lambda = 1, 10$, the truncation outage of mmWave networks experience a slow growth region as the cutoff threshold increases before its saturation contrary to UHF networks, which does not experience a slow growth region. The slow growth region is due to the difference in the truncation outage probability for LOS and NLOS links at a given cutoff threshold. Meanwhile, for a high BS density of $\lambda = 100$, the truncation outage probability of mmWave converges to that of UHF with $\alpha = 2$ since more paths becomes LOS as the BS density increases. As expected, Fig. 1

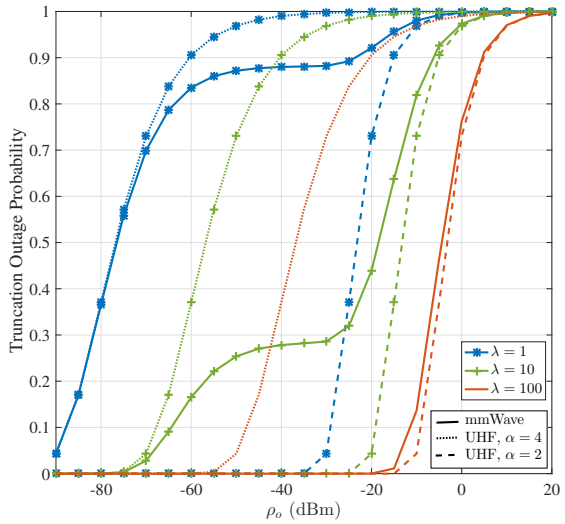


Fig. 1: Comparison of the truncation outage probability of mmWave and UHF cellular network

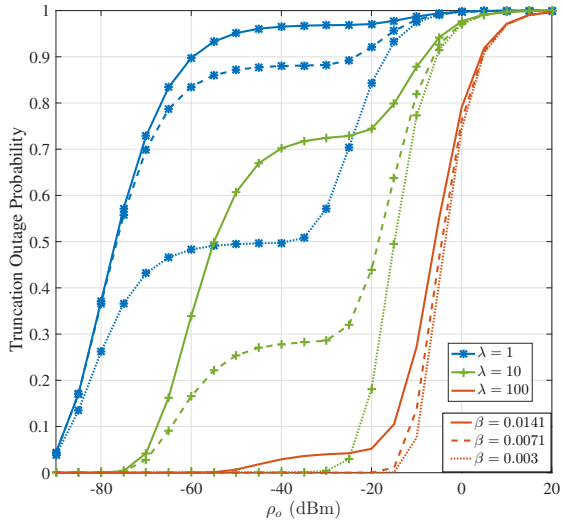


Fig. 2: Effect of the blockage parameter on the truncation outage probability.

shows that the truncation outage of mmWave networks reduces with as the BS density increases. This observation is due to the shortening of the average link lengths as the BS density is increased. Fig. 2 shows the effect of blockages on the truncated outage proabability. As the average line of sight increases the truncation outage probability reduces as much lower transmit power is required to meet the receiver sensitivity requirement when the density of blockages and average size of blockages are much lower.

In Fig. 3, we plot the SINR outage probability for the uplink of mmWave networks with truncated channel inversion power control for SINR threshold $\theta = 20, 25$ and $30$dB, and BS densities $\lambda = 1, 10$ BS/km$^2$. The results show that our derived analytical model accurately captures the SINR outage probability for mmWave cellular networks. Further, similar to the truncated outage probability, the SINR outage probability of mmWave deviates from that of the UHF network presented in [9]. More specifically, four sections can be identified from the plot for the BS density $\lambda = 10$ BS/km$^2$: 1) a decrease in

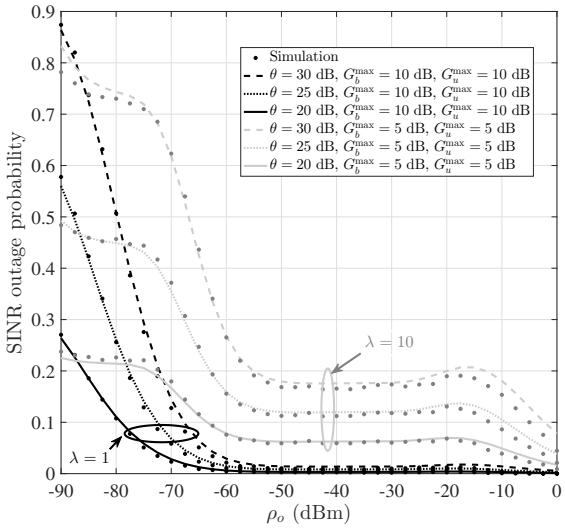


Fig. 3: SINR outage probability for $\sigma^2 = -110$ dBm,SINR threshold $\theta = 20, 25, 30$ dB and BS density $\lambda = 1, 10$ BS/km$^2$.

SINR outage probability can be seen for the cutoff threshold $\rho_o$ ranging from $-90$ to $-50$ dBm with a slow descent region observed for $\rho_0$ ranging from $-85$ to $-75$ dBm; 2) a fairly stable outage probability can be observed for $\rho_o$ ranging from $-50$ to $-31$ dBm; 3) an increase in SINR outage probability can be seen for $\rho_o$ ranging from $-31$ to $-18$ dBm, and 4) a decrease in SINR outage probability can be seen for $\rho_o$ ranging from $-18$ to $0$ dBm. This observation is as a result of the large difference in the pathloss exponent of the LOS and NLOS propagation path, with each having its dominance region which also depends on the BS density and blockage parameter. The latter specifies the LOS range. Further, the receiver sensitivity also specifies the density of active LOS and NLOS UEs and consequently, the interference received at the reference BS. It can also be observed from Fig. 3 that for the same SINR threshold, increasing the BS density leads to an increase in the SINR outage probability.

## VI. Conclusions

In this paper, we have presented a stochastic geometry framework to analyze the truncation outage probability and SINR outage probability in the uplink of millimeter wave (mmWave) cellular networks. The framework take the effect of blockages, the per-user equipment (UE) power control as well as the maximum power limitations of the UE. Further, each UE controls its transmit power such that the received signal at its serving base station is equal to predefined cutoff threshold $\rho_o$. Based on the proposed framework, we derived the expressions for the truncated outage probability and the signal-to-interference-and-noise-ratio (SINR) outage probability for the uplink of mmWave cellular networks. Numerical results show that contrary to the conventional ultra-high-frequency networks there exists a slow growth region for the truncated outage probability. Furthermore, increasing the cutoff threshold does not necessarily lead to a reduction in the SINR outage probability of the mmWave networks.


## Acknowledgement

We acknowledge the support of EPSRC (GCRF) funds under the grant no. EP/P028764/1.

## REFERENCES


[1] T. Rappaport, S. Sun, R. Mayzus, H. Zhao, Y. Azar, K. Wang, G. Wong, J. Schulz, M. Samimi, and F. Gutierrez, "Millimeter wave mobile communications for 5G cellular: It will work!" *IEEE Access*, vol. 1, pp. 335–349, 2013.

[2] T. Rappaport, F. Gutierrez, E. Ben-Dor, J. Murdock, Y. Qiao, and J. Tamir, "Broadband millimeter-wave propagation measurements and models using adaptive-beam antennas for outdoor urban cellular communications," *IEEE Trans. Antennas Propag.*, vol. 61, no. 4, pp. 1850–1859, Apr. 2013.

[3] S. Rangan, T. Rappaport, and E. Erkip, "Millimeter-wave cellular wireless networks: Potentials and challenges," *Proc. IEEE*, vol. 102, no. 3, pp. 366–385, Mar. 2014.

[4] M. Akdeniz, Y. Liu, M. Samimi, S. Sun, S. Rangan, T. Rappaport, and E. Erkip, "Millimeter wave channel modeling and cellular capacity evaluation," *IEEE J. Sel. Areas Commun.*, vol. 32, no. 6, pp. 1164–1179, Jun. 2014.

[5] Z. Pi and F. Khan, "An introduction to millimeter-wave mobile broadband systems," *IEEE Commun. Mag.*, vol. 49, no. 6, pp. 101–107, Jun. 2011.

[6] W. Roh, J.-Y. Seol, J. Park, B. Lee, J. Lee, Y. Kim, J. Cho, K. Cheun, and F. Aryanfar, "Millimeter-wave beamforming as an enabling technology for 5G cellular communications: Theoretical feasibility and prototype results," *IEEE Commun. Mag.*, vol. 52, no. 2, pp. 106–113, Feb. 2014.

[7] T. Bai and R. Heath, "Coverage and rate analysis for millimeter-wave cellular networks," *IEEE Trans. Wireless Commun.*, vol. 14, no. 2, pp. 1100–1114, Feb. 2015.

[8] T. Novlan, H. Dhillon, and J. Andrews, "Analytical modeling of uplink cellular networks," *IEEE Trans. Wireless Commun.*, vol. 12, no. 6, pp. 2669–2679, Jun. 2013.

[9] H. ElSawy and E. Hossain, "On stochastic geometry modeling of cellular uplink transmission with truncated channel inversion power control," *IEEE Trans. Wireless Commun.*, vol. 13, no. 8, pp. 4454–4469, 2014.

[10] O. Onireti, A. Imran, M. Imran, and R. Tafazolli, "Energy efficient inter-frequency small cell discovery in heterogeneous networks," *IEEE Trans. Veh. Technol.*, vol. 65, no. 9, pp. 7122–7135, Sep 2016.

[11] J. Zhang, L. Xiang, D. W. K. Ng, M. Jo, and M. Chen, "Energy efficiency evaluation of multi-tier cellular uplink transmission under maximum power constraint," *IEEE Trans Wireless Commun*, vol. 16, pp. 7092–7107, Nov 2017.

[12] O. Onireti, A. Imran, and M. A. Imran, "Coverage analysis in the uplink of mmwave cellular network," in *European Conference on Networks and Communications (EuCNC)*, Jun 2017, pp. 1–6.

[13] ——, "Coverage, capacity and energy efficiency analysis in the uplink of mmwave cellular networks," *IEEE Trans. Veh. Technol.*, vol. PP, no. 9, pp. 1–1, 2017.

[14] J. Andrews, A. K. Gupta, and H. S. Dhillon, "A primer on cellular network analysis using stochastic geometry," Apr 2016, [Online]: Available: http://arxiv.org/abs/1604.03183.

[15] T. Bai, R. Vaze, and R. Heath, "Analysis of blockage effects on urban cellular networks," *IEEE Trans. Wireless Commun.*, vol. 13, no. 9, pp. 5070–5083, Sep. 2014.

[16] D. Maamari, N. Devroye, and D. Tuninetti, "Coverage in mmwave cellular networks with base station co-operation," *IEEE Trans Wireless Commun*, vol. 15, no. 4, pp. 2981–2994, Apr 2016.

[17] H. Alzer, "On some inequalities for the incomplete Gamma function," *Math. Comput.,*, vol. 66, no. 218, pp. 771–778, Apr. 1997.

[18] J. Andrews, F. Baccelli, and R. Ganti, "A tractable approach to coverage and rate in cellular networks," *IEEE Trans. Commun.*, vol. 59, no. 11, pp. 3122–3134, Nov. 2011.